PUBLICATIONS OF THE ASTRONOMICAL SOCIETY OF THE PACIFIC, **119**: 255–258, 2007 March
© 2007. The Astronomical Society of the Pacific. All rights reserved. Printed in U.S.A.

Faint Objects at High Galactic Latitudes in the Sloan Digital Sky Survey

J. B. HUTCHINGS

Herzberg Institute of Astrophysics, Victoria, BC, Canada; john.hutchings@nrc.ca

AND

P. CHAYER AND L. BIANCHI

Department of Physics and Astronomy, Johns Hopkins University, Baltimore, MD; chayer@pha.jhu.edu, bianchi@pha.jhu.edu

Received 2007 February 2; accepted 2007 February 21; published 2007 March 2

ABSTRACT. We derive an empirical conversion of SDSS point sources to *J* magnitudes, in addition to resulting estimates of guide stars available to *JWST*. We also discuss high Galactic latitude fields in the SDSS in terms of completeness limits and populations of stars, galaxies, and QSOs.

1. INTRODUCTION

This work was triggered by the need to assess the guide stars available to the *James Webb Space Telescope* (*JWST*) using a guide camera that is sensitive in the near-infrared. The guide star catalog to be used is the GSC 2, which is currently used for the *Hubble Space Telescope* and is based on the Schmidt telescope optical sky surveys. In order to design the *JWST* guider (fine guidance sensor [FGS]) with sufficient field of view to have a 95% probability of having one guide star in the NIR, it was necessary to get some estimate of the stellar types and sky density at the Galactic poles. The FGS can guide on stars as faint as $J_{AB} = 19.4$.

The Sloan Digital Sky Survey (SDSS) and Two Micron All Sky Survey (2MASS) databases are ideal for this conversion to provide an estimate of *J* magnitudes and spectral types for objects beyond the 2MASS flux limits (see e.g., Finlator et al. 2000; Stoughton et al. 2002; Skrutskie et al. 2006). This conversion is described in the next section, along with the guiding consequences for *JWST*. The SDSS database goes several magnitudes fainter than the FGS guide star limit and includes some major apparent populations of faint objects. We discuss the nature and properties of these faint objects and what may be understood about them in the database.

2. *J*-MAGNITUDE ESTIMATES

Fields of 1° radius were selected at eight different Galactic latitudes and longitudes. The SDSS and 2MASS catalogs were retrieved for all of them. The positions of all objects were cross-correlated to match those in common, and joint catalogs were created. The separation criterion was that the positions agree to within 2″. In less than 1% of the cases, there were more than one within this radius, and the closest pair was chosen. Using these, various color-color plots were made (such as $J - g$ against $g - z$) to derive the transformation equations from SDSS filters to *J*. The transformation from *g* and *z* is $J = g - 0.59 - 1.54(g - z) + 0.20(g - z)^2 - 0.04(g - z)^3 + 0.002(g - z)^4$, and $J_{AB} = J + 0.9$. While *z* has less precision than *i*, it lies closer to *J* and produces a more robust conversion. Figure 1 shows the derived and 2MASS *J* magnitudes for two of the fields. The scatter is a good measure of the accuracy of the conversion. The bright objects are subject to inaccuracies of saturation, and those so flagged in the SDSS database were removed from the sample. Among the fainter stars, the scatter is slightly larger for blue objects ($g - i < 1$). The standard deviation of the scatter rises from ±0.09 mag at $J_{AB} = 16$ to ±0.2 at 18 mag. We estimate that this rises to about 0.5 mag at $J_{AB} = 19.4$.

It is possible to derive *J*-magnitude estimates from other SDSS filters. In particular, we looked at using *i* instead of *z*, as the *z* magnitudes are less reliable for fainter stars, being at the edge of the CCD sensitivity. On the other hand, the $g - i$ wavelength lever is shorter than that of $g - z$. The *J* magnitudes derived from *r* and *i* magnitudes show the same groupings of objects in the color-magnitude plots, so there is no systematic change of faint *J*-band accuracy for these alternative calibrations. However, comparison of *J* magnitudes from filters shortward of *z* all show a double-population, which tends to smear out the comparison of derived *J* magnitudes, getting worse as the wavelengths get shorter. Thus, we use the $(g - z)$-band calibration for the discussion but note that we have verified that our discussion is not affected systematically by using the other filters to derive the *J* magnitudes.

The high Galactic latitude star counts are estimated using the fields centered at longitude 150°, latitude 80°, and longitude 180°, latitude 70° and 80°. The lowest star counts occur at the last of these: looking slightly away from the Galactic pole and away from the Galactic center. The SDSS photometry was retrieved from the DR5 release (Adelman-McCarthy et al. 2007). We excluded from our analysis magnitudes with satu-

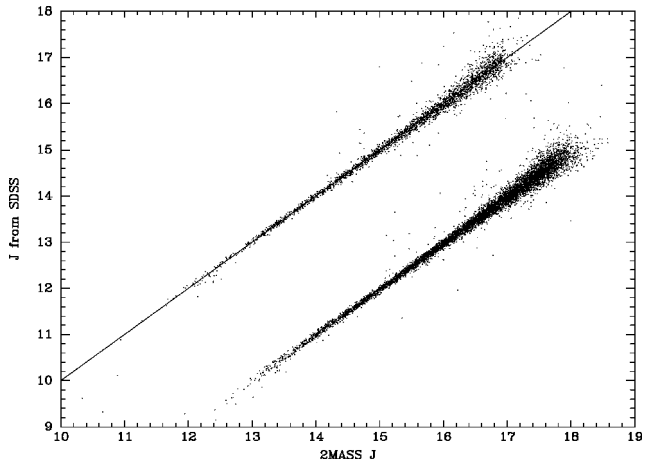

FIG. 1.—Comparison of J magnitudes from 2MASS and those computed from SDSS g and z filters. Two different fields are shown, with the points offset for one to enable comparison.

ration flags and edge flags. The SDSS pipeline generates faint spurious sources (e.g., Bianchi et al. 2007), the majority of which can be removed by cuts on photometric errors in the sample. The SDSS catalogs were edited to include only those flagged in the SDSS database as point sources with g errors of less than 0.5 mag and i errors of less than 0.4 mag. This eliminates essentially all the false sources. Figure 2 shows color-magnitude diagrams for point sources in two fields in the SDSS, in g and i, and the derived J magnitudes against $g - z$ for the lowest count field ($l = 180°, b = 80°$). We show the stellar spectral types corresponding to $g - z$ values as taken from standard stars in the SDSS catalog by Smith et al. (2002). Sources that are classified as extended (and thus are galaxies) have a different distribution, with a single maximum with color, peaking at $(g - i) \sim 1.2$. We discuss these later and show them in Figure 5.

There is a dense band of faint, unresolved ("point source") objects that is increasingly present as we move away from the direction of lowest density in the sky, seen in Figure 2. The *JWST* guide star limit of $J_{AB} = 19.4$ is brighter than this densely populated band of objects, and we can confidently assume they are stars that are potentially suitable for guiding. We discuss the distribution of spectral types and the guiding performance in the next section. In the subsequent section (§ 4), we discuss the nature of the fainter sources.

3. GALACTIC HALO STARS

Figure 2 shows the conversion from $g - z$ to spectral type. There are two distinct populations, which are seen down to $J_{AB} = 19$. If we bin the stars down to the guide limit by spectral type (Fig. 3), we can see that there are essentially none earlier than type G, and most are M0 and later. Moving 10° away in the sky adds about 600 M stars to the distribution, while the

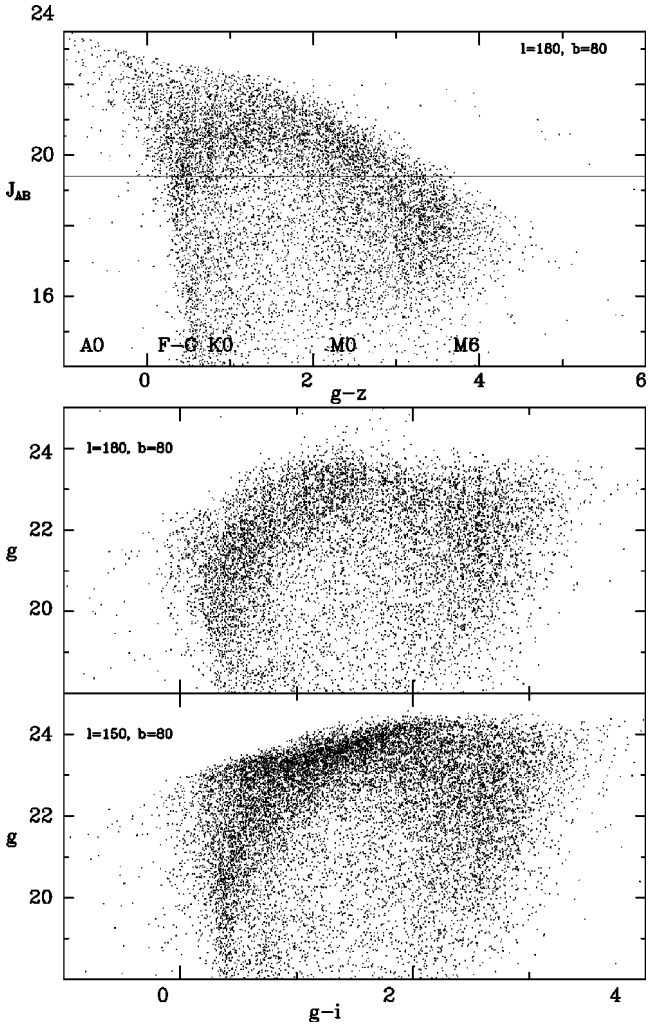

FIG. 2.—Color-magnitude plots in AB magnitudes for high-latitude fields. *Top*: J magnitudes computed from SDSS filters with $g - z$ for the $l = 180°$, $b = 80°$ field. Spectral types are shown for the $g - z$ values. The line at $J = 19.4$ is the *JWST* guide star faint limit. *Middle*: g magnitudes with $g - i$ for the same field. *Bottom*: Field at $l = 150°$, $b = 80°$. These are all unresolved sources, with g and i error bar limits of 0.5 and 0.4 mag, respectively, and all edge-flagged objects removed.

counts of earlier spectral types are almost unchanged. This has implications for guiding and also tells us something about the populations in the Galactic halo.

For guiding, the FGS detectors are bare HgCdTe detectors, with response from 0.8 to 5 μm. The FGS+detector signal from different spectral types is shown in Figure 4. This includes the telescope and instrument optical coatings, the detector response, and the star spectral energy distribution (SED). In order to estimate the guiding precision, we need to combine the point-spread function (PSF) shape (which depends on wavelength) with the signal level across all wavelengths, correctly weighted. In addition, there are values for read noise, Poisson noise, and centroiding box size that determine the limiting signal (and

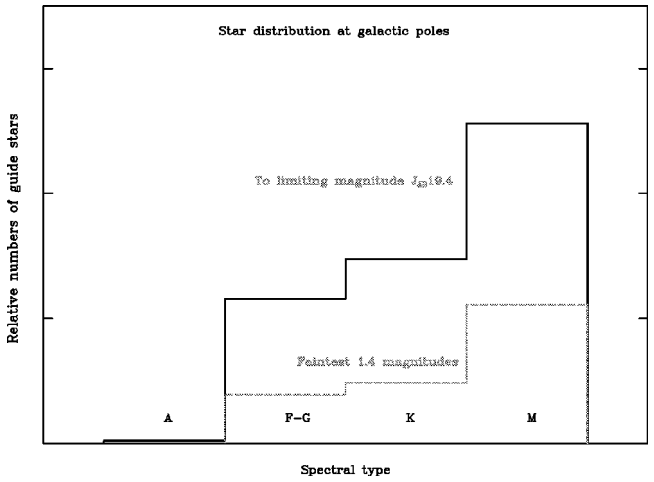

FIG. 3.—Distribution of spectral types to *JWST* guide star limit for the $l = 180°$, $b = 80°$ field, where star counts are lowest. The dashed histogram is for the faintest 1.4 mag of guide stars. Moving 10° away, the M star counts increase by about 0.6 units, while the others are close to the same.

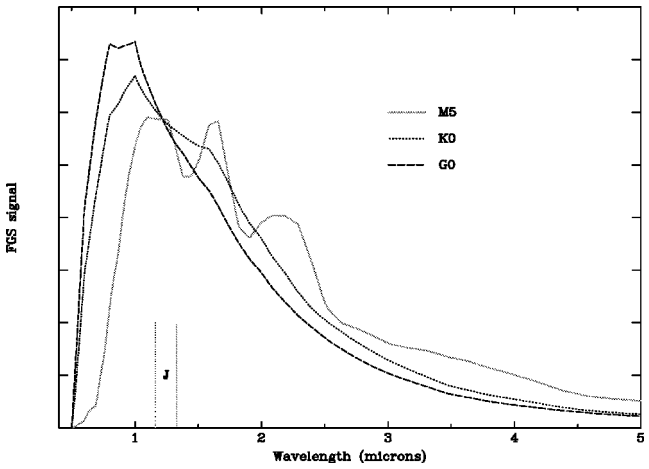

FIG. 4.—FGS signal level with wavelength for the range of guide star spectral types. The curves are normalized at the *J*-band wavelength. The total guide signal is the sum from 0.8 to 5 μm.

hence star magnitude) for the FGS. Thus, the distribution of star colors, as well as the number counts, determine the performance of the FGS guider.

In terms of stellar populations, the two distributions are assumed to be local M dwarfs and the general population of the Galactic halo, seen mainly as the G to K giants.

At the lowest star density point, the SDSS sample indicates that there are 6.3 stars brighter than the guide limit per single (5.5 arcmin^2) FGS field, and 3.9 stars per field that are 1.4 *J*-band magnitudes brighter than this. Ten degrees away in the sky, we have 0.8 additional M stars per field. These numbers assure guide star availability far in excess of the 95% level that is required for *JWST* (average of three per field). While many of these are not in the guide star catalog, it would be feasible to generate such catalogs for the low–star-density parts of the sky using a new dedicated *J*-band imaging program.

4. FAINT POPULATIONS

It is of interest to understand the nature of the fainter sources that show up in these high-latitude fields, as they may represent a mix of stellar populations in the Galactic halo and distant extragalactic objects. Figure 2 shows faint limits determined by the error bars in g and i. Figure 5 shows the distribution of point and extended sources from a high-latitude field. The extended sources (galaxies) occupy a space with a broad mix of $g - i$ colors up to $(g - i) \sim 2.5$. We compared the color distribution of our sources to model colors of stars, galaxies, and QSOs (models described in Bianchi et al. 2007). Stars with $T_{\rm eff}$ between 7000 and 4000 K occupy the same locus as galaxies and QSOs in the $(g - i)$-$(g - r)$ color-color diagram, while cooler stars (with $g - i > 2$) are well separated, having bluer $g - r$ than the red galaxies. Stars hotter than ~4000 K, and galaxies that share the same range of $g - i$ colors, separate in $u - g$. However, imposing detection in the u band significantly limits the sample of redder stars, due to the large u-band errors for red objects. However, most point sources can be considered stars (or QSOs), so galaxies can be separated using their spatial extent, with the likely exception of the fainter ones. There are essentially no or very few stars hotter than ~7000 K in this field.

Richards et al. (2004) discuss QSO populations in the SDSS

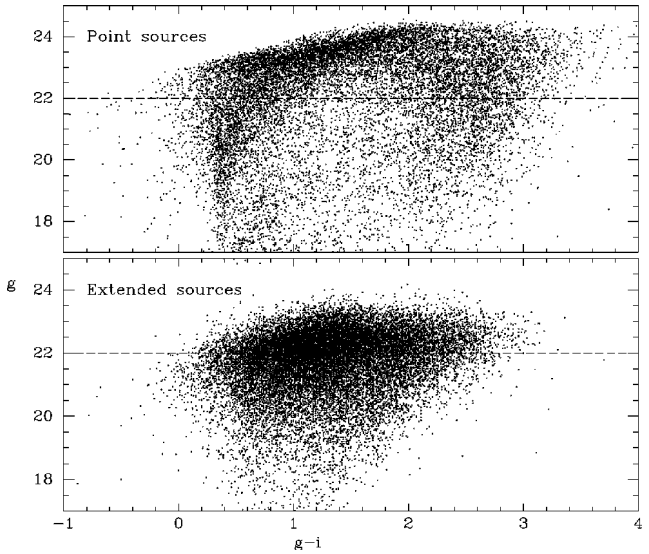

FIG. 5.—Plots of point and extended sources from the high-latitude field $l = 150°$, $b = 80°$, showing the different distributions. The dashed line at $g = 22$ in both panels is to aid visual comparison of the two distributions. The band of faintest point sources is surmised to be faint galaxies not resolved with SDSS imaging.

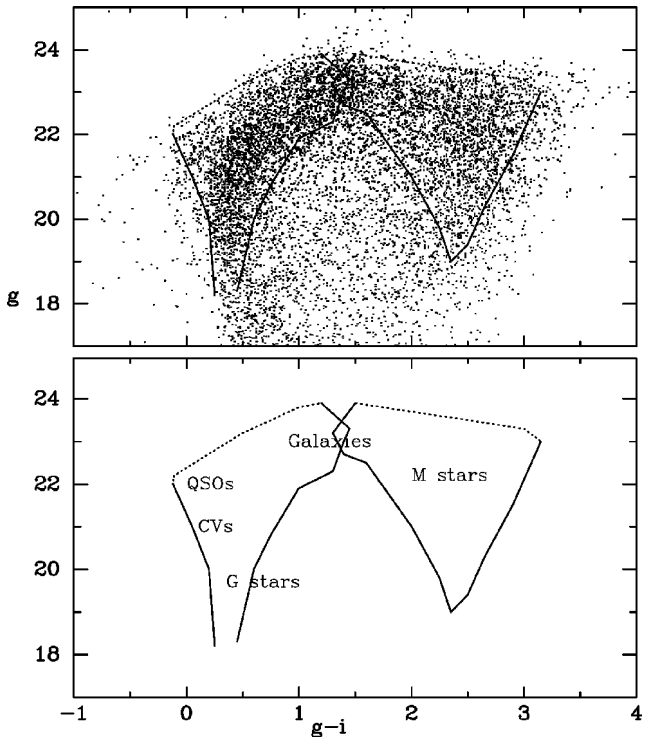

FIG. 6.—Same as Fig. 2 (*bottom panels*). The top panel contains the same points as Fig. 2 (*middle*). The outlined areas represent the loci of objects identified as labeled. The dotted lines indicate where incompleteness sets in. The brighter blue objects are F–G giants in the halo. The Galaxy locus is defined by Fig. 5.

database, and Bianchi et al. (2007) have extended the discussion with the *GALEX* UV two-color data. The QSO sequence (with redshift) almost follows the stellar sequence in the $(g - i)$-$(g - r)$ diagram. Thus, QSOs cannot be separated from stars using these colors. The low-redshift QSOs separate from the stellar sequence in $u - g$, where main-sequence stars between 7000 and 10,000 K have $(u - g) \approx 1$, but low-redshift QSOs have $u - g$ around 0.0–0.5, according to our (Bianchi et al. 2007) QSO templates. This is confirmed by a small number of pointlike sources seen at $u - g = 0.5$ to 0.0 and $g - i = 0.0$ to 0.5, which roughly correspond to redshifts between 0 and 2. QSOs at higher redshift are hardly detected in the u band.

We have plotted the positions of QSOs and galaxies of known redshift from the SDSS spectroscopic database on color-magnitude diagrams and find that they occupy adjacent regions (QSOs slightly bluer), with $g - i$ 0 to 1 and magnitudes brighter than 20. See Figure 6 for a sketch and comparison with our lowest density field plots. We note that these are SDSS "point sources," so the galaxies must be compact or perhaps are the cores of larger galaxies. The SDSS spectra do not cover objects in the faint bands we are discussing here, but the galaxy locus seems likely to extend to redder color as they get fainter (and more redshifted), and very likely account for a good fraction of the densely populated central regions of the band (i.e., the blue end of the red band).

The distribution of faint M stars clearly extends into the red band, with $g - i$ colors becoming more spread out as photometric errors increase. Thus, we consider that the red band consists of this faint population extending to redder colors than faint galaxies. If we plot the mean magnitudes of objects in the red band from all the SDSS filters, they correspond very closely with that for M stars in the SDSS standard lists.

The bluest objects are probably mostly low-redshift QSOs, but may include hot white dwarfs or accretion-disk-dominated cataclysmic variables (CVs). It is interesting that these objects are rare at brighter magnitudes, and we will discuss this population further in a study of QSO candidates selected by Bianchi et al. (2007) from *GALEX* and SDSS databases (Hutchings et al. 2007, in preparation).

We thank Peter Stetson for useful discussions, and James Herald for helping with the database queries. Funding for the SDSS has been provided by the Alfred P. Sloan Foundation, the participating institutions, NASA, NSF, US Department of Energy, Japanese Monbukagakusho, and the Max Planck Society.

REFERENCES

Adelman-McCarthy, J. K., et al., 2007, ApJS, submitted
Bianchi, L., et al. 2007, ApJS, in press (astro-ph/0611926)
Finlator, K., et al., 2000, AJ, 120, 2615
Richards, G. T., et al., 2004, ApJS, 155, 257
Skrutskie, M. F., et al., 2006, AJ, 131, 1163
Smith, J. A., et al. 2002, AJ, 123, 2121
Stoughton, C., et al., 2002, AJ, 123, 485